Investigation of consolidation mechanisms induced by applied electric/electromagnetic fields during the early stages of spark plasma sintering

Anis Aliouat, Guy Antou, Nicolas Pradeilles, Vincent Rat, Alexandre Maître

Investigation of consolidation mechanisms induced by applied electric/electromagnetic fields during the early stages of spark plasma sintering

Anis Aliouat [1], Guy Antou [1,*], Nicolas Pradeilles [1], Vincent Rat [1], Alexandre Maître [1]

[1] ***Univ. Limoges, CNRS, IRCER, UMR 7315, F-87000 Limoges, France***

* *Correspondence: guy.antou@unilim.fr*

Abstract

This work aims at investigating the role of the electric/electromagnetic fields generated by the pulsed current applied during Spark Plasma Sintering (SPS) process on the sintering mechanisms. The selected model material was a metallic granular medium composed of microsized particles of pre-oxidized copper. Its electrical behavior and correlated microstructural modifications were studied in two complementary enclosures. First, a demonstrator equipped with a modulable pulsed electric current generator has allowed analyzing, at low temperature and without mechanical loading, the effects related to the application of an electric wave, by controlling and modulating its characteristics (*i.e.* shape, frequency, amplitude). An abrupt electrical transition, named "Branly effect" from an insulating to a conductive state, is observed in the granular copper medium. The increase of pulses frequency is shown to strongly reduce the critical time to generate the electrical transition. Moreover, a commercial SPS device, with specific electrical and thermal instrumentation, was implemented by varying applied stress and using conductive and insulating dies. The analysis of the electrical behavior coupled with *post-mortem* microstructural observations allowed to highlight that the coupling between pulsed current and mechanical stress promotes specific mechanisms in SPS. Under high stress, interparticle contact area increase and the insulating oxide layer is damaged by microcracking. The coupling with the flow of the pulsed current involves local overheating and dielectric breakdown, favoring ignition of Branly effect. Micro-welds are formed between particles, creating privileged paths of the pulsed current and initiating densification at low temperature (250 °C).

Keywords: metals and alloys (A); sintering (B); dielectric response (B); electrical transport (B); microstructure (B); scanning electron microscopy, SEM (D).

1. Introduction

Spark Plasma Sintering (SPS), also known as electric-discharge sintering or field-assisted sintering technique (FAST), is an unconventional and promising sintering method for producing dense materials with a fine microstructure and exceptional performance [1–4]. This technique is based on the simultaneous application of a uniaxial stress (10-100 MPa) and a high heating rate (up to 1300 °C/min) [5,6]. This latter is induced by an applied pulsed electric current within the graphite tooling [2], or even in the granular medium (if it is conductive) [7]. This process allows densifying granular compact in very short times and at lower sintering temperatures (up to several hundred degrees) than those applied in presssureless sintering [8]. Moreover, SPS makes it possible to sinter refractory materials [9,10], difficult to densify by conventional techniques, such as carbides (tungsten carbide [11,12], boron carbide [13–15], zirconium carbide [16,17]) and nitrides (boron nitride [18], silicon nitride [19], aluminum nitride [20]).

However, all the physical phenomena generated by the applied pulsed current are still not fully understood. In particular, the role of the electromagnetic (EM) fields induced by the pulsed feature of the current is generally reduced to the generation of heat by Joule effect at the macroscopic scale. However, only a few studies try to address the effects induced by the EM fields, which can significantly contribute to the improvement of the densification process [21–23]. Some specific effects associated with applied EM fields during SPS treatment are mentioned, such as electromigration (*i.e.* diffusion motion of the metallic ions by promoting the electric field during the SPS) [5,24,25], crystallographic texture [26], microstructural inhomogeneity in thermoelectrics caused by Peltier effect-induced temperature gradient [27,28], local overheating [29,30], surface cleaning by dielectric breakdown [31,32], or Branly effect [22,33].

Over the last few years, copper has been the main topic of many studies in the literature to better understand the EM-induced effects during SPS of conductive metal powders. This interest stems from three main characteristics of this unique material [4]: (i) it does not undergo any phase transition and is densified by solid state sintering; (ii) its oxides are easily destabilized during the sintering process; (iii) its remarkable electrical properties make it an ideal candidate to study the densification mechanisms of conductive powders.

Among the specific effects presumed in SPS, previous studies on copper have suggested the existence of phenomena of local overheating and cleaning of the oxide layer on the surface of the copper particles during the early stages of SPS process. Yanagisawa *et al.* [29] studied the morphology of necks formed at the interfaces between spherical copper particles of mondispersed size distribution (diameter of 550 μm) subjected to an electrical discharge. They reported the formation of micro-bridges and necks between the copper particles, whose morphology suggests local

melting. Under these conditions, extremely high temperatures are reached by the generation of local heat at the interparticle contacts. This local overheating would explain the fusion and/or evaporation of copper at the points of contact between the particles. According to them, this phenomenon could occur during the initial phase of sintering, *i.e.* when the contact surface and the relative density are low. Using a similar approach, Diouf *et al.* [34] also observed similar non-conventional melted bridges between copper particles (a few millimeters in diameter) during SPS at 900 °C. In this regard, the local overheating was theoretically and experimentally investigated by Song *et al.* [30] on spherical pure copper powder with range of diameter of 15-40 μm. Based on their experiments, the authors observed the formation of fine grains in the neck zones at relatively low sintering temperatures (from 440 to 880 °C). It suggests that neck is formed through a local melting and the subsequent rapid solidification. Through analytical calculations, they suggested that the generated heat is distributed inhomogeneously from the particle-contacting surface toward the core. The highest temperature is estimated at the surface of the particle (*i.e.* the contact region of the two particles) and can reach 3000 °C (higher than the copper boiling point). These authors concluded that this local overheating induced by the passage of current at the interparticle contacts leads to the formation of necks at relatively low sintering temperatures by combining local melting and rapid solidification. The effect of the electric current on the SPS process was also studied by Zhang *et al.* [35] on pure copper particles having an average size of about 2.5 μm, sintered for 5 min at 600 °C under 50 MPa. Based on SEM observations, they proposed that the morphology of formed necks would be typical of a transition to the liquid state followed by projection of matter. According to them, the interparticle necks develop due to a process of evaporation–condensation following by the splashing of molten copper between the surfaces of the particles. Besides, other studies suggested dielectric breakdown as a mechanism for cleaning the particle surfaces during SPS based on SEM and TEM observations. The surface cleaning process was observed and highlighted on copper particles during SPS treatment by Wu *et al.* [32]. From TEM examinations, they showed that the boundaries between copper particles consolidated were clean. Indeed, the oxide layer would be removed from the surface of Cu powders and repelled to the triple junctions, which leads to the formation of clean Cu-Cu interface. They suggested that the localized high temperature produced by the electric field concentration at interfaces between copper particles is the dominant mechanism for surface cleaning. Similarly, Bonifacio *et al.* [31] suggested that the dielectric breakdown can cause surface cleaning on Ni particles covered with an ultra-thin NiO oxide layer (thickness of 2 nm) during SPS. These authors have used *in situ* TEM to replicate the processing conditions during SPS and to directly observe surface cleaning. They have shown that the removal of surface oxides of Ni particles occurs through electric field-induced dielectric breakdown. Furthermore, in our previous investigation [22,33], it has been reported that the Branly effect can probably occur during the early SPS stages due to inductive effects generated by

the applied pulsed current. The Branly effect corresponds to an electrical transition from an insulating to a conductive state that appears in a metallic powder, slightly oxidized on the surface, under the application of an electric or EM field. The generation of the Branly effect can promote the consolidation of the granular medium, through the destruction of the insulating oxide layer at interparticle contacts and the formation of micro-bridges.

In contrast to those previous works, Collet *et al.* [36] claimed that there is no surface cleaning effect of copper particles induced by the pulsed current applied during SPS. Their experiment consisted of sintering three pure copper powders, showing different oxide layer thicknesses and an average diameter of 25 µm. The same sintering conditions were applied in Hot Pressing (HP) and SPS (heating rate of 25 °C/min, dwell temperature of 900 °C and a pressure of 4 MPa). From their SEM analyses on the fractured parts of the samples, no significant microstructural discrepancies were observed between the SPS and HP treated samples. They reported that the surface oxide layer is pushed away from the interparticle contacts and forms "collars" around the necks. By increasing the stress applied to 28 MPa in SPS [37], they observed a lowering of the temperature from which the oxide is "repelled" from the interfaces, this occurring between 500 and 700 °C depending on the thickness and of the composition of the native oxide layer. According to them, this is due to the applied mechanical pressure and the temperature, without the effect of the pulsed electric current.

The presence of specific electric and electromagnetic effects enhancing the densification mechanisms in the early stage of the SPS process is hence the subject of controversy in the literature. To understand well the consolidation mechanism during SPS, this work aims to deconvolute the phenomena associated with the different physical fields applied during SPS treatment: the temperature, the mechanical stress applied, the electric current and the electromagnetic wave potentially generated by the pulsed character of the current. To dissociate the multiple physical fields encountered in SPS, two complementary enclosures associated with specific electrical generators will be used. First, a demonstrator equipped with a modulable pulsed electric current generator will allow studying the behaviour of a granular medium composed of micrometric pre-oxidized copper particles submitted to a pulsed electric current of high amperage. The shape of the applied electric wave will be controlled and modulated. The effects related to the passage of pulsed currents at several frequencies will be analyzed at low temperature without mechanical loading. Then, a commercial SPS device will be used to investigate the combined effects of temperature and mechanical stress to the imposed electric and magnetic fields. A specific thermal and electrical instrumentation will be used to monitor the electrical behavior of the copper powder. The tooling will be adapted in order to force or not the passage of the pulsed current within the powder bed. The microstructural modifications and their evolution induced by the flow of current will be finely characterized by electron microscopy (SEM-FIB).

2. Materials and Methods

2.1. *Raw powder*

The copper powder selected to perform this study was a commercial powder "Metco 55" provided by Sulzer Metco Europe GmbH (Germany). This powder was already used in our previous works [22,33], and its structural and morphological properties have been finely characterized. It was obtained by a gas atomization process and exhibits micro-sized spherical particles. The raw powder was sifted using stainless-steel sieves of 70 µm and 112 µm in order to tighten its particle size distribution and thus have the most monodispersed particles as possible. It leads to an average volume diameter of about 87.5 µm. This powder has a chemical purity higher than 99.5%. The main impurity consists of tin dioxide (SnO_2). It is pre-oxidized and has an oxygen content of about 0.27 wt.%. A thin oxide layer with a thickness of 1.2 µm covers the surface of the copper particles. This oxide layer is mainly composed of crystallized Cu_2O oxide, with the presence of CuO at the extreme surface of the particles.

2.2. *Demonstrator equipped with a modulable pulsed electric current generator*

The electrical behavior of the copper powder is studied using a demonstrator equipped with a pulsed electric current generator. This generator can deliver a pulsed current of high amperage, up to 6 kA under a maximum voltage of 6 V. The pulsed wave applied by this device can be modulated in terms of shape, frequency and amplitude. Particular attention will be paid here to the influence of the frequency of the applied current wave on the induced electrical transition and the associated microstructural modifications. The objective is to study and highlight the potential EM effects induced within the granular stack by the pulsed character of the current, with current peaks reaching several hundred amperes in a few milliseconds.

The experimental setup is presented in ***Figure 1A***. It consists of two stainless steel electrodes mounted on a frame, the upper electrode (*i.e.* upper plunger) being mobile. The copper powder is poured into a die of 10 mm diameter, and is located between two graphite spacers (themselves in contact with the electrodes). The stress applied to the powder bed is very low (3.8 MPa), corresponding to the weight of the upper plunger and the graphite spacer (total weight of 30.6 kg). The tooling and the sample are placed in a sealed enclosure, which operates in air at atmospheric pressure.

The pulsed current generator has been specifically designed by CERA - Schneider Electric (Eybens, France), and allows controlling the characteristics of the current wave (shape, frequency,

amplitude and number of pulses) thanks to an integrated software. However, the frequency of the wave is limited to a few tens of Hertz, and is thus slightly lower than the typical frequency of the pulsed current applied by commercial SPS machines, of about 300 Hz for the Dr. Sinter-type devices supplied by Fuji company [38]. During these experiments, the setpoint chosen for the current wave have a triangular shape. The amplitude of the current wave is fixed at 325 A. Two pulse duration setpoints are applied: 14 ms and 140 ms. The programmed current is compared to the current really delivered by the generator. ***Figure 1B*** and ***Figure 1C*** show the comparison between the setpoint currents and those delivered by the generator. In both cases, as expected, the delivered current does not follow the programmed setpoint. For the 14 ms duration setpoint, the current wave delivered is not perfectly triangular (***Figure 1B***). Moreover, the duration of the pulses is approximately 25 ms, leading hence to a frequency of the pulses of 40 Hz. For the higher pulse duration setpoint at 140 ms (***Figure 1C***), the current wave has a quasi-square shape with a maximum amplitude of 115 A. The programmed pulse duration is fairly well respected and is actually around 160 ms, resulting in a current wave frequency of 6 Hz.

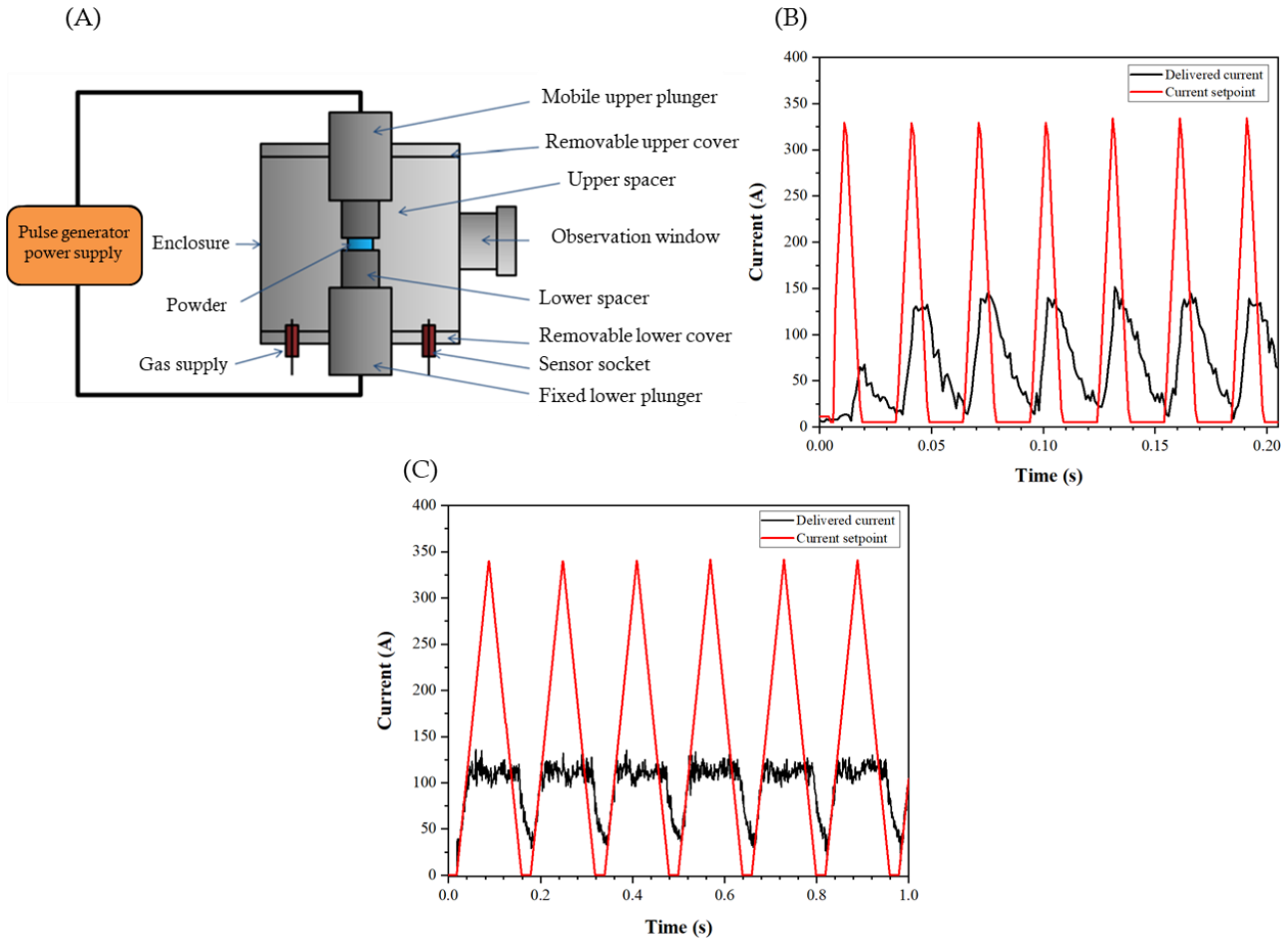

Figure 1: Schematic of the pulsed current demonstrator (A); delivered current pulses with actual frequencies of 40 Hz (B) and 6 Hz (C).

The copper powder is poured into the die to form a powder bed of 0.30 mm thickness. The experiments are performed at room temperature and under atmospheric pressure. All electrical measurements are repeated five times to ensure good reproducibility of results. The tests are performed using two types of die:

- a conductive graphite die: in this case, the pulsed current is conducted through the die, and also flows through the sample if it is conductive (***Figure 2A***).
- an insulating die, *i.e.* a graphite die whose internal wall is covered with a thin layer of boron nitride (0.2 to 0.3 millimeters thick) by spraying. This layer of BN is electrically insulating, and its presence forces the pulsed current to flow through the sample (***Figure 2B***). Before each test, the insulating character of the BN layer is checked by a resistance measurement between the die and the plungers.

Finally, a thermocouple is introduced into the die, and is positioned as close as possible to the sample (distance of 5 mm). It allows following the temperature variations within the sample during the tests.

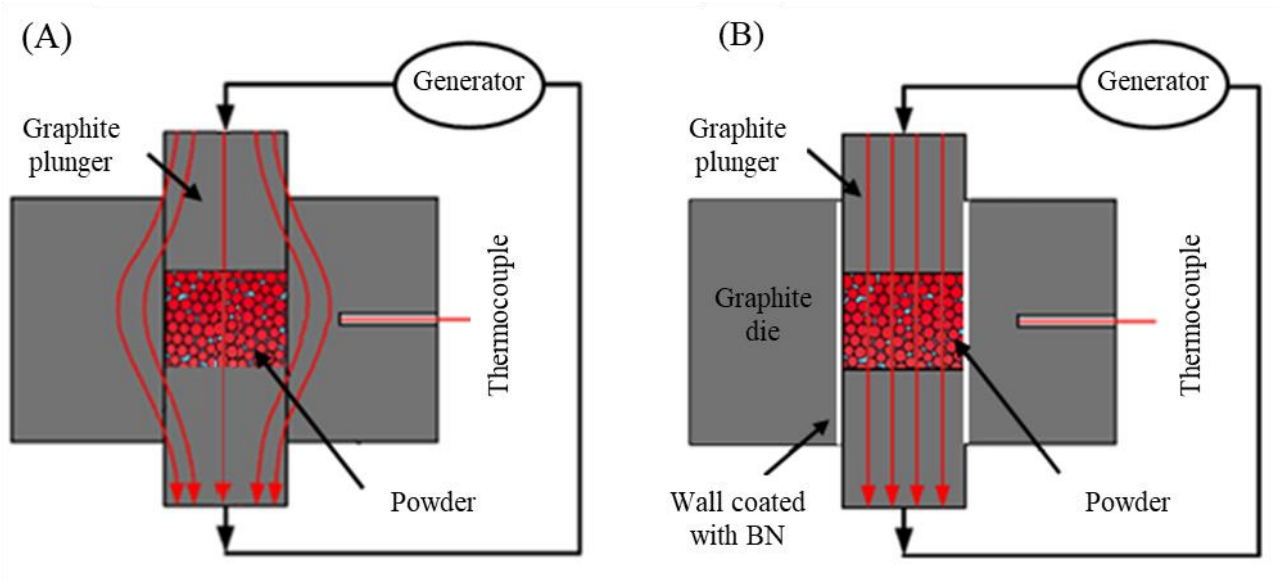

Figure 2: Schematic representations of the two experimental configurations used during measurements with the pulsed current demonstrator: (A) conductive die; (B) insulating die.

2.3. *SPS experiments*

SPS experiments are also performed to investigate how the applied temperature and mechanical stress affect the behaviour of the powder under pulsed current. A commercial SPS device (model Dr. Sinter SPS 825, Fuji Electronics Industrial Co.Ltd., Japan) is used. This device is capable of delivering a maximum average current of 8 kA and a maximum voltage of 15 V. Specific electrical and thermal instrumentations have been implemented in the SPS machine [38]. Measurement of the

instantaneous electrical potential applied to the SPS column is achieved by using two stainless steel electrodes (150 mm diameter and 0.5 mm thick discs) placed between Inconel electrodes of the machine and graphite spacers. These electrodes are used to measure the voltage pulses applied to the ends of the SPS column. To instantaneously measure the intensity of the delivered pulsed current, a Rogowski loop (model CWT60, Power Electronic Measurements Ltd, England) is placed, without contact, around the copper plates (rectangular section with a width of about 30 cm and a thickness of 2 cm) of the SPS machine. A temperature measurement is performed with a K-type thermocouple, positioned on the external surface of the die (halfway up). Measured temperatures, current intensity and voltage are collected through a data acquisition card (NI cDAQ-9174 with three CRIO-9215 type modules, National Instrument, France) by using a LabView acquisition program. The sampling frequency is fixed at 30 kHz in order to accurately describe each pulse whose frequency is about 300 Hz (for the Dr Sinter-type SPS apparatus, as the duration of a single pulse is around 3 ms). Nevertheless, during SPS treatments, heating is regulated on the temperature measurement, but not on the applied current. The data processing is conducted using an acquisition program developed under Labview (National Instrument, Nanterre, France). The default pulse waveform of 12:2 (on:off) is applied (***Figure 3***). It corresponds to a sequence of 12 pulses (3.3 ms each) "on" and (2×3) 6 ms with no current (off). The frequency of the elementary current pulses is hence approximately of 300 Hz.

A first series of tests are performed with a Teflon insulating die using an internal diameter of 10 mm and a wall thickness of 5 mm. The thickness of the powder bed is again fixed at 0.30 mm. The minimum load applicable (*i.e.* 3.2 kN, equivalent to a uniaxial compression of 41 MPa) by the hydraulic cylinder of the SPS device is retained.

In addition, SPS tests using a more standard graphite tooling configuration are carried out in a conductive graphite die with an internal diameter of 40 mm and a wall thickness of 15 mm. The thickness of the powder bed in this case is 5 mm. Two levels of uniaxial stress are applied: low loading tests with an applied uniaxial stress of 2.5 MPa and high loading tests with an applied uniaxial stress of 125 MPa. The heating and cooling rates are fixed at 50 °C/min up to 250 °C, with a dwell time of 5 min. All SPS treatments are achieved under a vacuum of about 10 Pa.

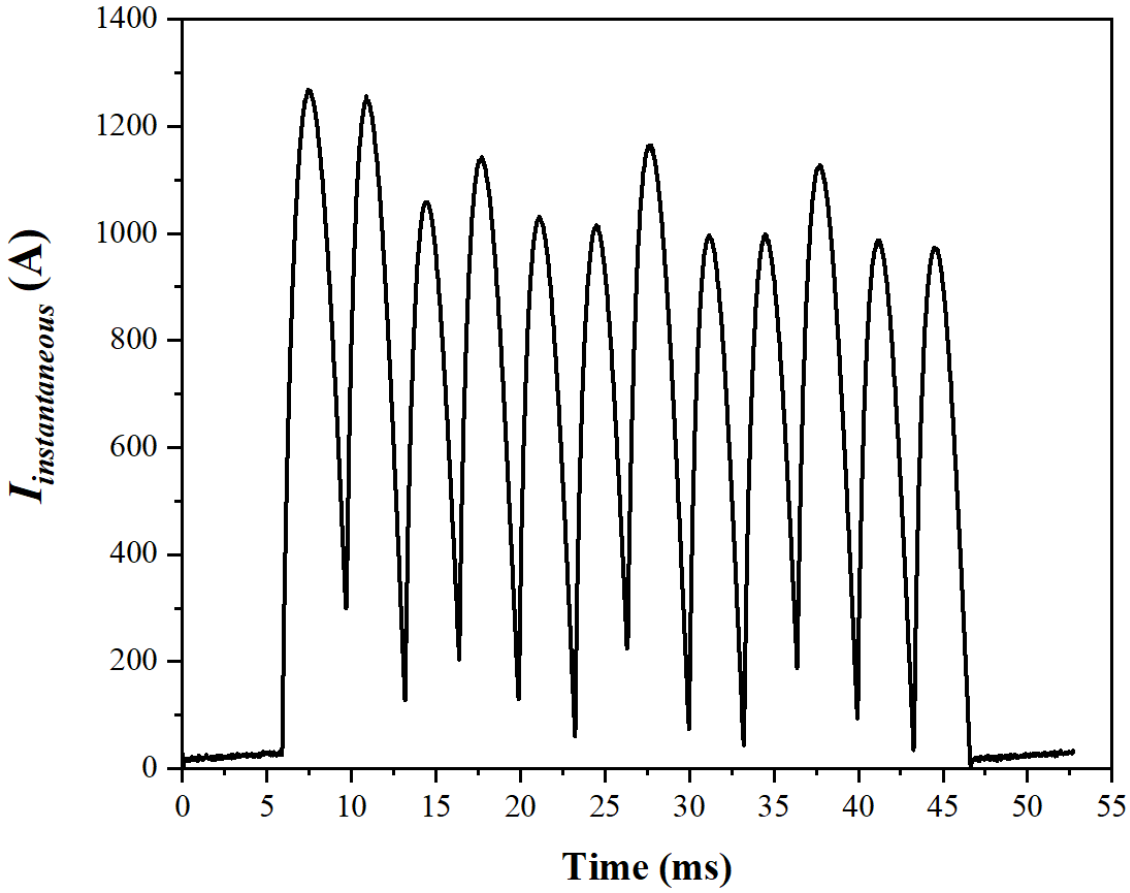

Figure 3: Typical instantaneous current recorded for a 12-2 pulse sequence during SPS treatment.

3. Results and Discussion

3.1. *Electrical measurements with the pulsed current demonstrator*

I) Tests with a conductive die

First, an experiment is conducted by pouring the copper powder in a conductive graphite die, which corresponds to the standard tooling configuration in SPS process. The frequency of the pulsed current is set at 40 Hz. ***Figure 4*** shows the temporal evolution of the RMS current (I_{RMS}) and instantaneous current ($I_{\text{instantaneous}}$). As soon as the voltage is applied (with a maximum amplitude of 6 V), the pulsed current flows with current peaks around 44 to 60 A, leading to an initial RMS value of 36 A. The total duration of the test is 15 s. A progressive and slow increase of the delivered RMS current is noted, going from 36 A to 43 A after 15 s. This small increase of the RMS current seems to be related to a slight heating by Joule effect, the measured temperature reaching 100 °C at the end of the test.

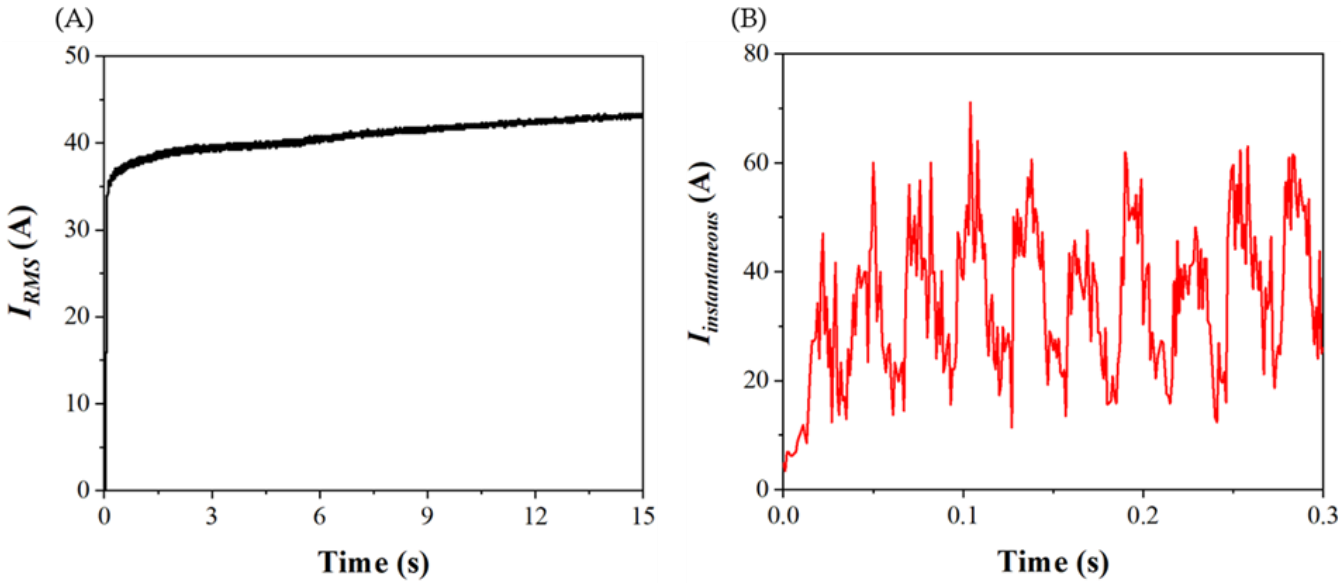

Figure 4: Temporal evolution of RMS current (A) and instantaneous current (B) when applying a pulsed current at a frequency of 40 Hz using a conductive die.

II) Effect of the pulse frequency (using an insulating die)

In order to promote the electromagnetic effects induced by the pulsed character of the current, the copper powder is poured into an insulating die (*i.e.* graphite die insulating thanks to a thin BN layer deposited on its inner wall). Its electrical behaviour is compared when submitted to pulsed currents of variable frequencies. The purpose of this insulation of the die is to force the pulsed current to circulate only in the copper powder. ***Figure 5*** shows the electrical measurements obtained when pulsed currents at frequencies of 6 and 40 Hz are applied.

For a frequency of 40 Hz, at the beginning of the test (***Figure 5A*** and ***Figure 5B***), the measured RMS current is almost null, the current values being very low and below the detection threshold of the current sensor. This low current flow during the first few seconds would be due to the insulating character of the copper powder which results from the presence of a thin oxide layer on the surface of the copper particles (the initial electrical resistance of the granular medium with a thickness of 0.30 mm being about 22 ± 5 MΩ [33]). Then, when a critical time (t_c) of about 6 s is reached, the RMS current increases sharply and suddenly, current peaks oscillating between 65 and 90 A. This marks the abrupt electrical transition from an insulating to a conducting state of the granular medium. Close observation of the evolution of instantaneous voltage (***Figure 5C***) shows that the peak voltage value rises from 3.25 V to 6.0 V at the moment of transition. This transition, known as the Branly effect, is marked by a significant drop in the electrical resistance of the granular medium by several orders of magnitude [22,33,39]. After the electrical transition, the flow of the pulsed current of high amperage (I_{RMS} = 55 A) in the sample leads to a progressive increase in temperature (direct heating of the

powder by Joule effect). However, the temperature at the end of the test remains moderate, around 55 °C. This test was repeated five times using the same experimental procedure. For all the tests, the abrupt electrical transition appears very quickly, with an average critical time of 5 ± 4 s.

The frequency of the current pulses was decreased to 6 Hz (pulse duration of 160 ms), resulting in a reduction in frequency by a factor of 6. ***Figure 5D*** and ***Figure 5E*** show the measured electrical behaviour of the sample. Initially, the granular medium is insulating, and the current is almost zero. When a critical time of about 51 s is reached (for the test shown here), the RMS current increases sharply, with current peaks oscillating between 50 and 80 A. This marks the electrical transition initiated within the stack. The evolution of instantaneous voltage in ***Figure 5F*** shows that the peak voltage value rises from 4.5 V to 6.0 V at the moment of transition. By repeating this test five times, the critical transition time is 60 ± 25 s.

A comparison of the RMS voltages delivered by the tests at 40 and 6 Hz is shown in ***Figure 5G***. For the two tests presented here, the RMS voltages before transition are 2.3 and 2.7 V, at 40 and 6 Hz respectively. By repeating these two types of tests five times, the average RMS voltages recorded before transition are 2.1 ± 0.4 and 2.7 ± 0.1 V, at 40 and 6 Hz respectively. This corresponds to a voltage difference of 28 %. Despite this slight increase in voltage (before transition) at lower frequency, which induces a slight increase in power, the electrical transition appears for a much longer time.

Finally, the comparison of these tests performed at variable pulse frequencies (6 Hz *vs.* 40 Hz) highlights that the increase in frequency (by a factor of 6) clearly shortens, by one decade, the critical time needed for obtaining the electrical transition. These results clearly show that EM effects are induced by the pulsed character of the current and favors the acceleration of the electrical transition.

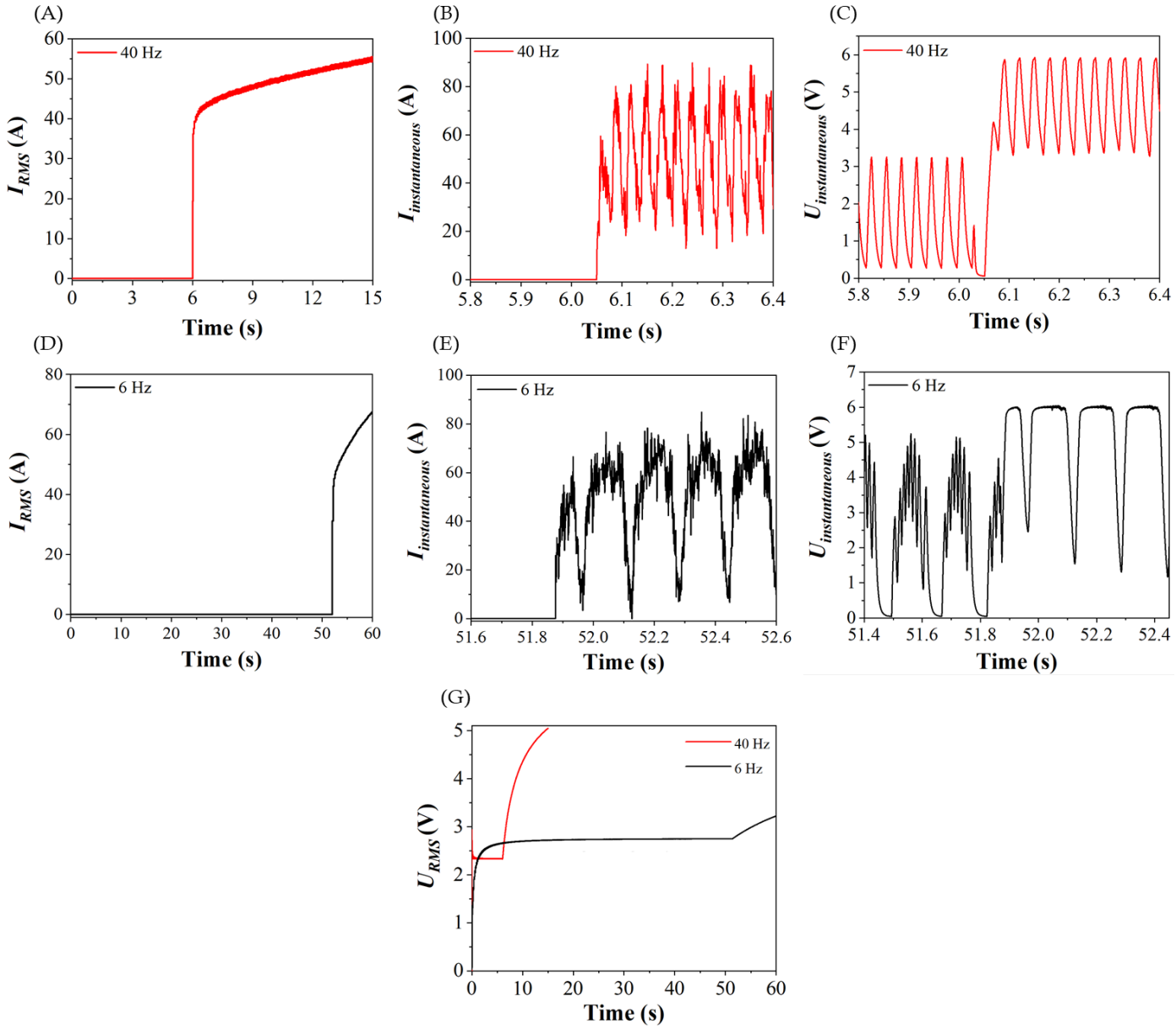

Figure 5: Application of pulsed currents of variable frequencies for copper powder in an insulating die: evolutions of the RMS current (A, D), of the instantaneous current at the moment of the electrical transition (B, E), of the instantaneous voltage at the moment of the electrical transition (C, F) and of the RMS voltage (G) for pulse frequencies of 40 and 6 Hz, respectively.

III) Microstructural observations

In order to well understand the microstructural changes induced by the flow of the pulsed current, careful post-mortem SEM investigations are carried out (***Figure 6***).

Figure 6A shows the SEM micrograph of the copper powder after application of a pulsed current at a frequency of 40 Hz for 15 s in a conductive die. Whatever the frequency of the current applied (40 Hz or 6 Hz), after application of the current, no clusters of particles are observed in the granular

medium, this latter remaining powdery. The surface of the particles is relatively smooth, and seems to have undergone no modification. In addition, no micro-bridges are formed between the copper particles, suggesting that the granular medium is still resistive and that the electrical transition has not been initiated. During this test, the pulsed current preferentially crosses the conductive die and leads to its slight heating by Joule effect. The copper powder remains insulating and undergoes an indirect heating by thermal conduction from the graphite tooling. This limited heating (temperature of 100 °C measured after 15 s) probably leads to a slight decrease in the electrical resistances of the sample and the graphite tool, explaining the gradual and slight increase in the measured RMS current (***Figure 4A***).

Figure 6B, ***C*** & ***D*** provide the SEM observations on the copper powder after holding the pulsed current at 6 Hz for 8 s after the electrical transition in an insulating die. At low magnification (***Figure 6B***), the presence of a highly consolidated cluster of copper particles is detected. At higher magnification (***Figure 6C***), the formation of micro-bridges at the inter-particle contacts is noticed. The size of these micro-bridges is 20 to 35 µm. Some of the copper particles show crater-like tearing marks on their surfaces. Within these tearing marks, the oxide layer is no longer present. Thus, the measured abrupt electrical transition is related to a strong local temperature rise at the inter-particle contacts by the applied pulsed current. Finally, this phenomenon leads to a local destroying effect of the oxide layer and the welding of the metal particles. In the literature, post-mortem observations of copper particles treated by SPS have highlighted this localized destruction of the oxide layer: a surface cleaning phenomenon is then evoked [30,31]. Around these micro-welds, the morphology of the oxide layer on the surface of some consolidated particles became rough (***Figure 6D***), suggesting a recrystallization of this layer under the effect of the circulation of the pulsed current of high amperage (I_{RMS} = 55 A). Moreover, in these strongly consolidated zones, the oxide layer remaining on the surface of the particles is strongly damaged and cracked (***Figure 6D***) as mentioned in the literature [30,34].

The microstructure obtained after transition on the copper powder after holding the pulsed current at 40 Hz in an insulating die is similar to the one observed here under pulsed current at 6 Hz. The micro-welds formed in the granular media have a morphology and an average size relatively similar to those already presented in ***Figure 6B & C***.

Whatever the imposed current frequency (40 Hz *vs*. 6 Hz), comparison of the microstructures obtained with conductive and insulating dies shows that a much longer current flow time with a conductive die (15 s in conductive die *vs.* 8 s after transition in insulating die) is not enough to initiate the electrical transition in the granular media and does not lead to the formation of micro-welds within the copper powder (***Figure 6A***). These tests, conducted under low mechanical loading (stress applied

of 3.8 MPa), lead to the generation of the Branly effect only by forcing the pulsed current to flow through the powder with an insulating die (***Figure 6B***, ***C*** & ***D***).

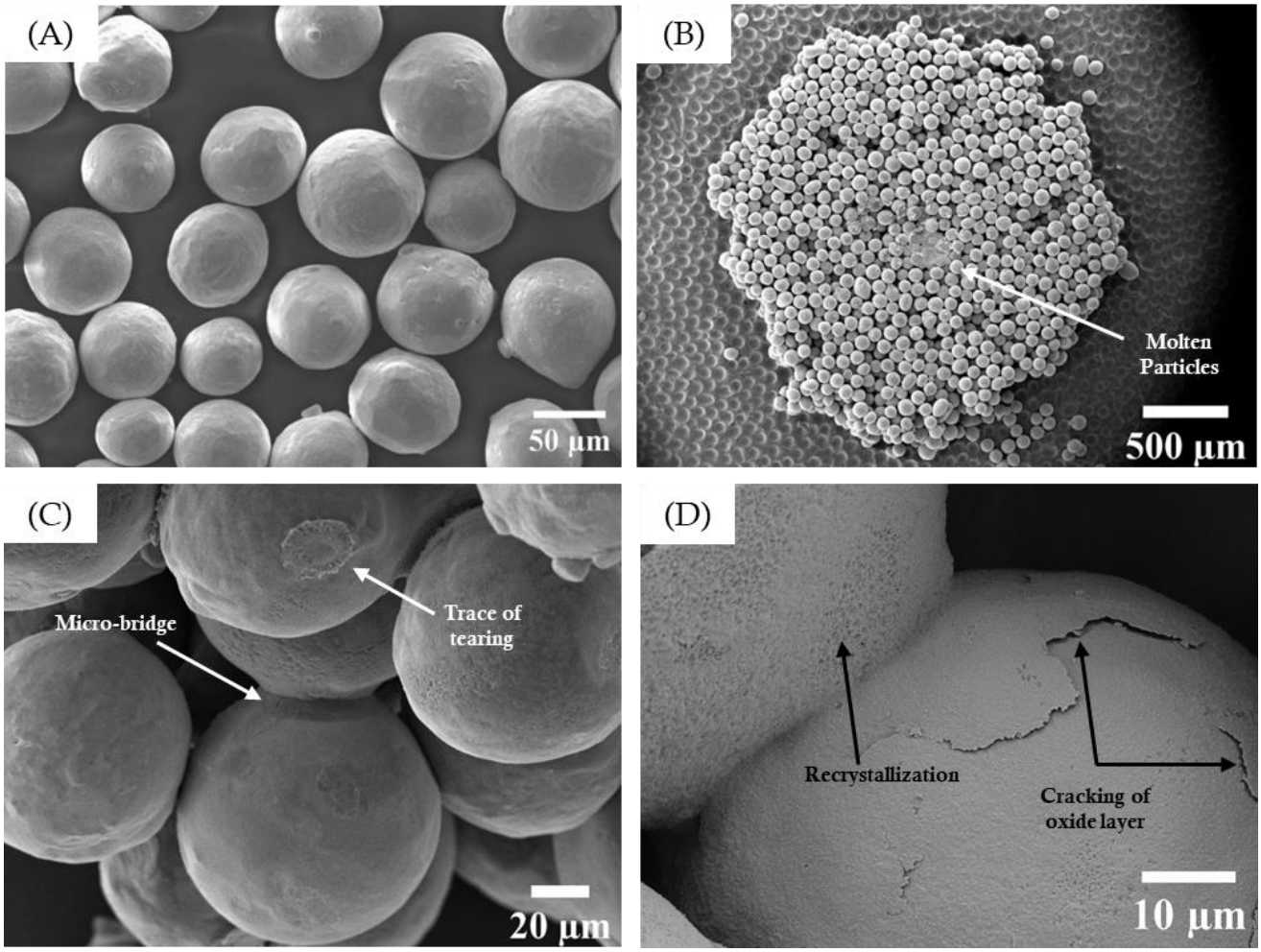

Figure 6: SEM micrographs of copper powder after application: (A) of a pulsed current at a frequency of 40 Hz for 15 s in a conductive die; (B, C & D) of a pulsed current at 6 Hz and holding the current for 8 s after the electrical transition in an insulating die.

3.2. *SPS treatments*

Tests conducted with the pulsed current demonstrator have shown that increasing the pulse frequency from 6 to 40 Hz promotes the ignition of the Branly effect and the formation of micro-welds between the copper particles. This result, highlighted by forcing the pulsed current to flow within the granular stack, suggests the existence of EM effects involved in the consolidation of copper particles. The frequency range imposed by the demonstrator is one decade lower than that of the pulses applied by commercial SPS machines of the Dr-Sinter type (supplied by Fuji Electronics Industrial Co. Ltd., Japan). The pulse frequency is higher, of approximately 300 Hz in SPS apparatus.

Consequently, this part aims at studying the electrical behavior of the copper powder and the consolidation mechanisms initiated during the early stages of SPS treatments. The coupling between mechanical loading and pulsed current is investigated by varying the applied stress level. The measured electrical behaviors are correlated to the microstructural evolutions observed by SEM.

I) Analysis of the transition time in SPS with the use of an insulating die

In an usual SPS treatment, the current flows through the tooling but also the powder depending on its electrical properties. In this section, first, an insulating die is used. It aims at forcing the current to flow through the copper powder in order to facilitate the detection of the critical time corresponding to the ignition of the electrical transition under pulsed current in SPS. A moderate stress of 41 MPa is applied to the powder bed. It allows analyzing the combined effects of mechanical pressure and EM effects induced by the pulsed character of the current in SPS, while limiting heating.

Figure 7 shows the electrical and thermal measurements obtained from the specific instrumentation during SPS of the copper powder using an insulating die. As shown by ***Figure 7A***, after 1 s, the RMS voltage of 0.6 V is not sufficient to initiate the electrical transition in the granular medium, leading to a near-zero current (lower than the measurement uncertainty of the current sensor). Then, the electrical transition of the granular medium (from an insulating to a conductive state) starts at 2 s, with RMS current and voltage values of 75 A and 2.4 V respectively. The current flows for 4 s (for 2 s < t < 6 s), with a maximum RMS current of 90 A. Heating begins with current flow at 2 s (***Figure 7B***). The maximum temperature recorded during the test is 60 °C.

A careful examination of the evolution of the measured instantaneous current at the time of the electrical transition is presented in ***Figure 7C***. Before the transition (t < 2.0 s), the current flowing in the granular medium is almost zero. From the first hundredths of seconds after the transition (between 2.0 and 2.1 s), the magnitude of the current pulses increases quickly: from 20 A to about 100 - 140 A.

Keeping an identical size of the granular stack (10 mm diameter and 0.3 mm thickness), the electrical transition time measured in SPS is clearly lower than the one measured with the pulsed current demonstrator: $t \approx 2.0$ s in SPS (with pulse frequency of 303 Hz under applied stress of 41 MPa) *vs.* $t \approx 5.0$ s in the demonstrator (with pulse frequency of 40 Hz under applied stress of 3.8 MPa). This comparison suggests that in SPS, the increase of the pulse frequency combined with the applied pressure significantly accelerates the ignition of the electrical transition (Branly effect).

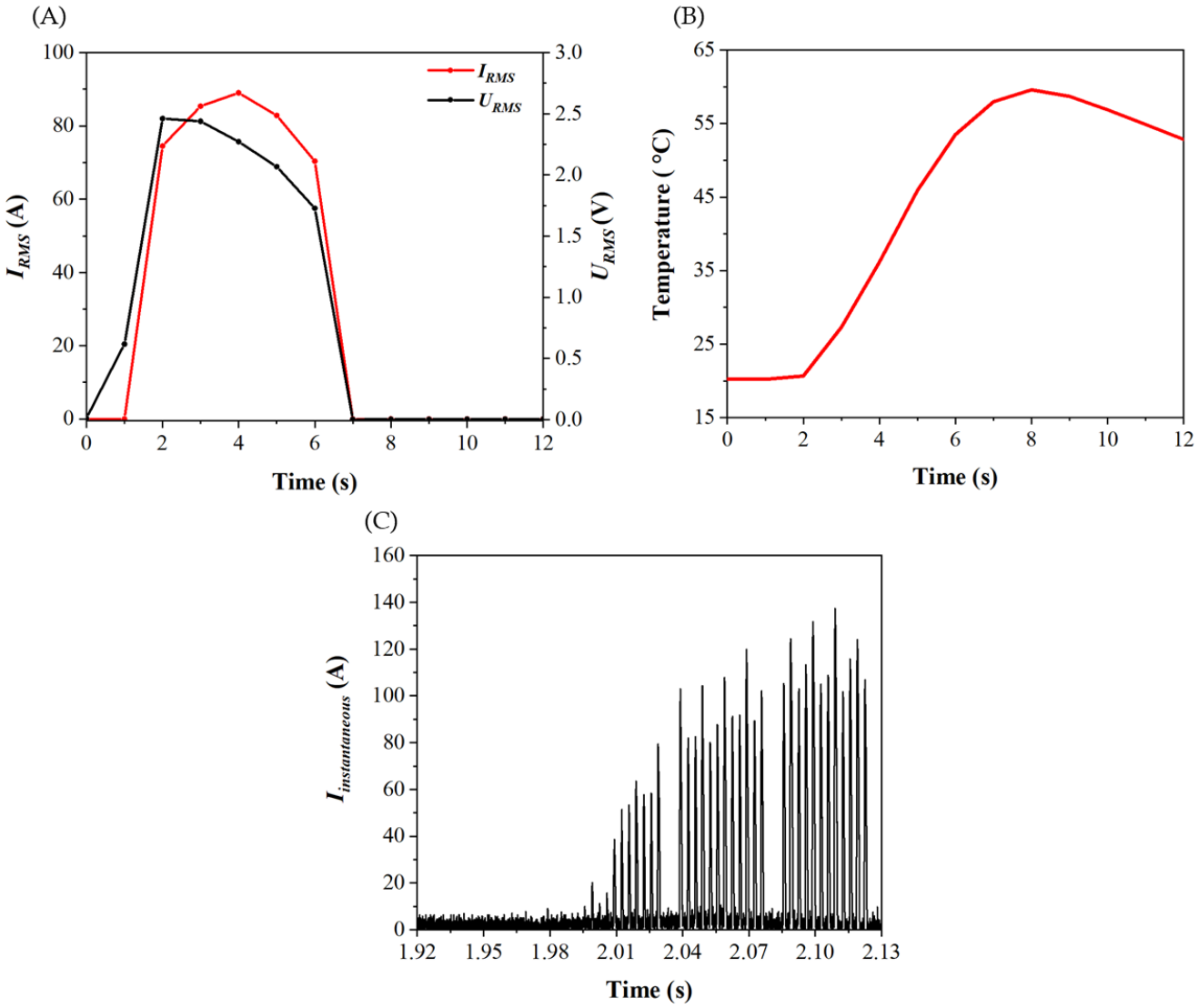

Figure 7: Measured evolutions of RMS current and voltage (A), temperature (B) and instantaneous current at the moment of the electrical transition (C) for copper powder treated by SPS in an insulating die (applied compressive stress of 41 MPa).

II) Coupling of mechanical stress and pulsed current with the use of a conducting die

The objective is here to highlight the coupling of the applied physical fields in SPS on the involved microstructural modifications.

These tests are conducted with a conductive graphite die of 40 mm diameter by varying the applied mechanical stress. It corresponds to the classical configuration of the SPS tooling. Given the minimum load of 3.2 kN that can be applied and regulated by the hydraulic cylinder of the SPS machine, this relatively large size of the die was chosen in order to allow the effect of the mechanical pressure to be investigated. Two levels of uniaxial stress are hence applied: low stress of 2.5 MPa (minimum load of 3.2 kN) and high stress of 125 MPa. For both stress levels, an identical thermal cycle is imposed, *i.e.* a ramp of 50 °C/min up to 250 °C, a temperature hold of 5 min before cooling

at 50 °C/min. The maximum temperature of 250°C was chosen to focus on the early stages of the SPS treatment, corresponding to the consolidation of the granular medium without any pronounced advancement of the densification process. Indeed, the smaller the size of the interparticle contacts and the relative density, the more the constriction effects associated with the pulsed current flow are predominant.

Figure 8A shows the measured evolutions of RMS current and temperature during SPS of the copper powder up to 250 °C under a low applied stress of 2.5 MPa. Upon application of the pulsed current, the current flows readily through the conductive die with an initial RMS current of 275 A. During heating (up to 300 s), the delivered RMS current gradually increases, with a maximum value of 1050 A at 300 s. In parallel, the temperature measured at the outer surface of the die increases almost linearly over the central range of the anisothermal regime. Just before the isothermal dwell (at 300 s and 220 °C), the RMS current is reduced to reach 250 °C after 400 s. Then, during the isothermal stage at 250°C, the RMS current is regulated and drops to 450 A at the end of the stage.

Figure 8B shows the measured changes in RMS current, stress and temperature during the SPS treatment of the copper powder up to 250 °C under a high stress of 125 MPa. Unlike the low stress test (under 2.5 MPa), the first phase of the treatment consisted of gradually increasing the stress to reach 125 MPa after 300 s, without heating. Then, from the beginning of the heating (after 300 s), the applied RMS current is about 450 A. It increases to reach an RMS value of about 1500 A just before the isothermal stage. During the anisothermal regime, the RMS current range is increased by about 50% compared to that imposed during the test at 2.5 MPa: 430 to 1500 A for 125 MPa *vs.* 275 to 1050 A for 2.5 MPa. The current delivered remains significantly higher during the isothermal stage. This discrepancy can be explained by the measured electrical resistances of the SPS column (tooling and powder) which are significantly lower during the test under high loading (≈ 1 mΩ under 125 MPa *vs.* ≈ 2 mΩ under 2.5 MPa). The lower electrical resistance of the column during the test under 125 MPa leads the servo system of the SPS machine to impose a higher current range to heat the assembly by Joule effect and reach the same setpoint temperature of 250 °C.

After treatment in the SPS device under 125 MPa, the sample is consolidated and has a final thickness of 3.76 mm (for a powder bed of 5 mm initial thickness). An electrical characterization by imposing a direct current cycle up to 1 A was conducted on the SPSed sample to measure its electrical properties, in particular its electrical resistance. The analysis shows that the treated sample has a very low electrical resistance (less than 1 Ω). This indicates that the granular compact has become conductive and that an electrical transition (Branly effect) occurred during the SPS treatment of the powder at 250 °C under 125 MPa.

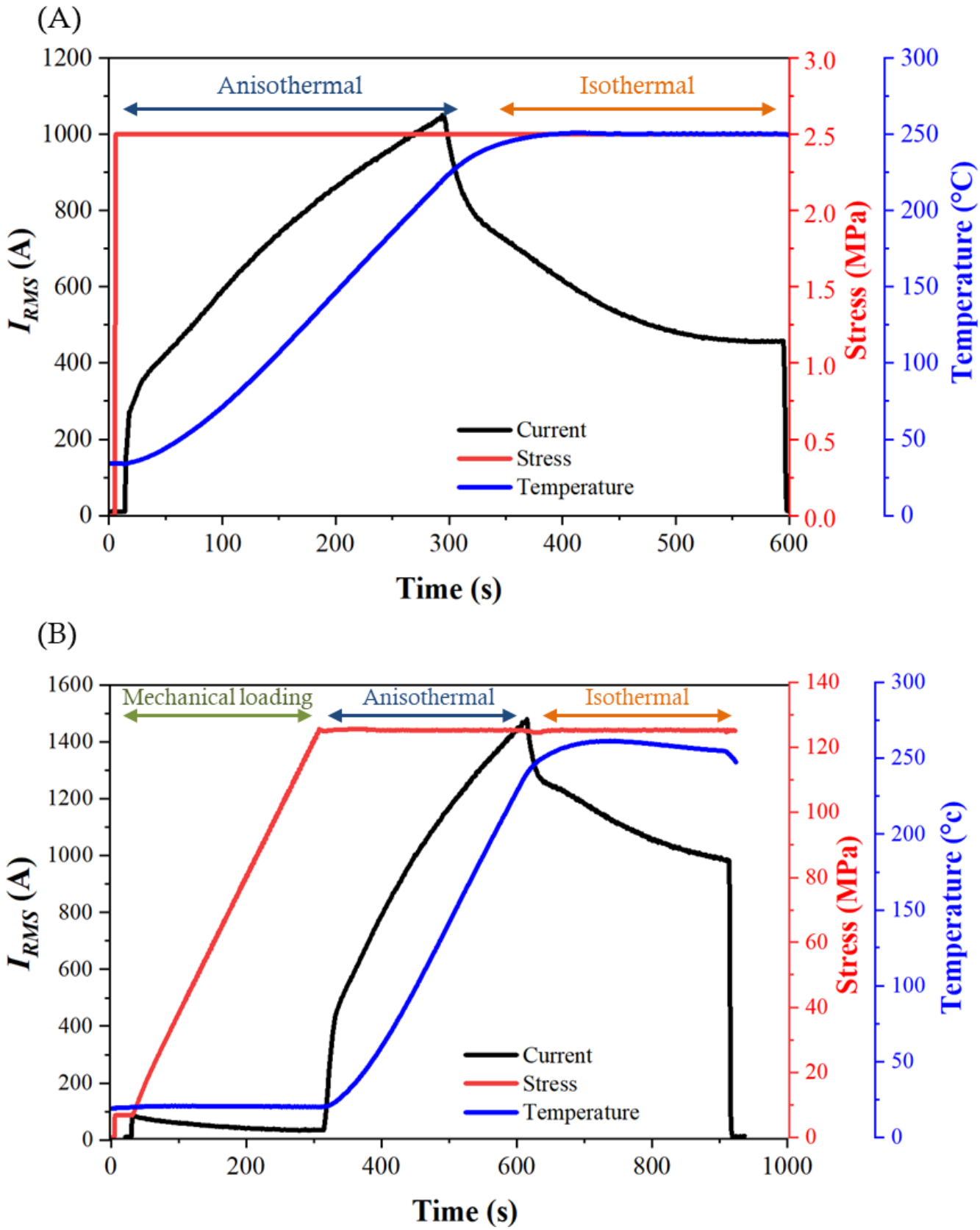

Figure 8: Evolutions of RMS current, stress and temperature during the SPS treatments of the copper powder up to 250 °C for 5 min (with a conductive die): (A) at low stress of 2.5 MPa; (B) at high stress of 125 MPa.

In order to analyze the effect of couplings between mechanical stress and EM fields applied in SPS, the SPSed sample is compared to a powder bed compacted at room temperature under the same uniaxial stress of 125 MPa. The final height of the SPSed sample at 250 °C under 125 MPa is lower than that of the cold compacted sample under the same stress (3.76 mm *vs.* 3.91 mm). Their final relative densities are 76.8 % and 73.9 %, respectively for the SPSed and cold compacted materials. This comparison shows that consolidation and densification phenomena are initiated by SPS under these conditions despite the imposed low dwell temperature (250 °C). The coupling between pulsed current and mechanical stress in SPS promotes the electrical transition of the copper powder and the early stage of the densification of granular compact.

III) Microstructure of SPSed samples

Microstructural observations by SEM are conducted after SPS to confirm the presence or absence of consolidation within the SPSed samples. ***Figure 9*** shows the SEM micrographs of the copper powder after SPS treatments with the conductive and insulating dies.

Using an insulating die, ***Figure 9A***, ***B*** & ***C*** show *post-mortem* SEM observations after achieving the electrical transition in the SPS device. In this experiment, the current flows for 4 s with a maximum RMS value of 90 A. At low magnification (***Figure 9A***), a cluster of molten particles is visible. The particles within this cluster appear to have been strongly consolidated and welded. At higher magnification (***Figure 9B***), outside the melted areas, micro-bridges have formed at the contacts between the copper particles. The size of these micro-bridges is about 40-50 µm. Inside the necks formed between the particles (traces of tearing visible on the surface of some particles, ***Figure 9B***), the oxide layer is destroyed, which leads to the formation of metallic micro-bridges between the particles. In addition, the surfaces of some particles show traces of fusion and liquid copper projection (***Figure 9C***). The particles are faceted due to the applied stress of 41 MPa (***Figure 9A***). The contact surfaces are flat and relatively circular in shape. The size of the necks formed (40 to 50 µm for a median particle diameter of 87 µm) indicates that, beyond the consolidation of the granular stack, the copper particles have begun to approach each other: this marks the beginning of the densification process of the powder.

The microstructure observed here after transition in the SPS device (with a maximum RMS current of 90 A for 4 s under 41 MPa) can be compared to that obtained after transition in the pulsed current demonstrator (with a maximum RMS current of 55 A for 8 s under 3.8 MPa). Microstructural observations after application of the pulsed current reveal significant melting in the SPSed sample and stronger consolidation compared to the sample treated in the pulsed current demonstrator. The

micro-welds formed between the particles are more numerous and larger. This comparison of microstructure reveals that a coupling of electro-magneto-thermo-mechanical phenomena operates in SPS. The intense local heating generated by the circulation of current pulses at the level of interparticle contacts is combined with the plastic deformation caused by the applied pressure. This coupling of multi-physical fields accelerates local deformation kinetics and promotes densification.

Using a conductive die under a low stress of 2.5 MPa (dwell temperature of 250 °C for 5 min), no consolidated clusters of particles are detected (***Figure 9D***). However, analysis at higher magnifications reveals the presence of a few micro-bridges formed at the interfaces between some particles (***Figure 9E***). The size of these micro-bridges is of the order of 10 µm. Thus, even if the material remains powdery at the macroscopic scale under these SPS conditions, the electrical transition seems to be initiated, at least partially in some areas of the granular stack.

Using a conductive die under a high stress of 125 MPa, the applied mechanical loading led to plastic deformation of the particles as revealed by the presence of faceted particles (***Figure 9F***). The contact surfaces are circular, with a diameter of about 30 µm. At higher magnification, consolidated clusters of particles with the presence of molten copper are present (***Figure 9G***). Micro-bridges and traces of tearing with a diameter of 25-30 µm are observed. At the level of these traces of tearing, the oxide layer is no longer present. They correspond hence to metal-to-metal links. Outside the consolidated zones marked by the presence of micro-bridges and traces of tearing, the unconsolidated particles are faceted without eliminating the oxide layer at the interfaces. At the facets of these particles, damage by microcracking of the oxide layer is observed both at the core of the facet and at its periphery (***Figure 9H***). This damage of the insulating oxide layer induced by the applied mechanical stress favors the ignition of the electrical transition, as shown in our previous work on the study of the Branly effect under low DC current and variable stress levels [33]. Finally, these SEM micrographs reveal that the SPS-induced micro-welds are not homogeneously distributed within the stack. Some particles faceted under the effect of pressure remain unconsolidated, with an oxide layer still present at the interfaces.

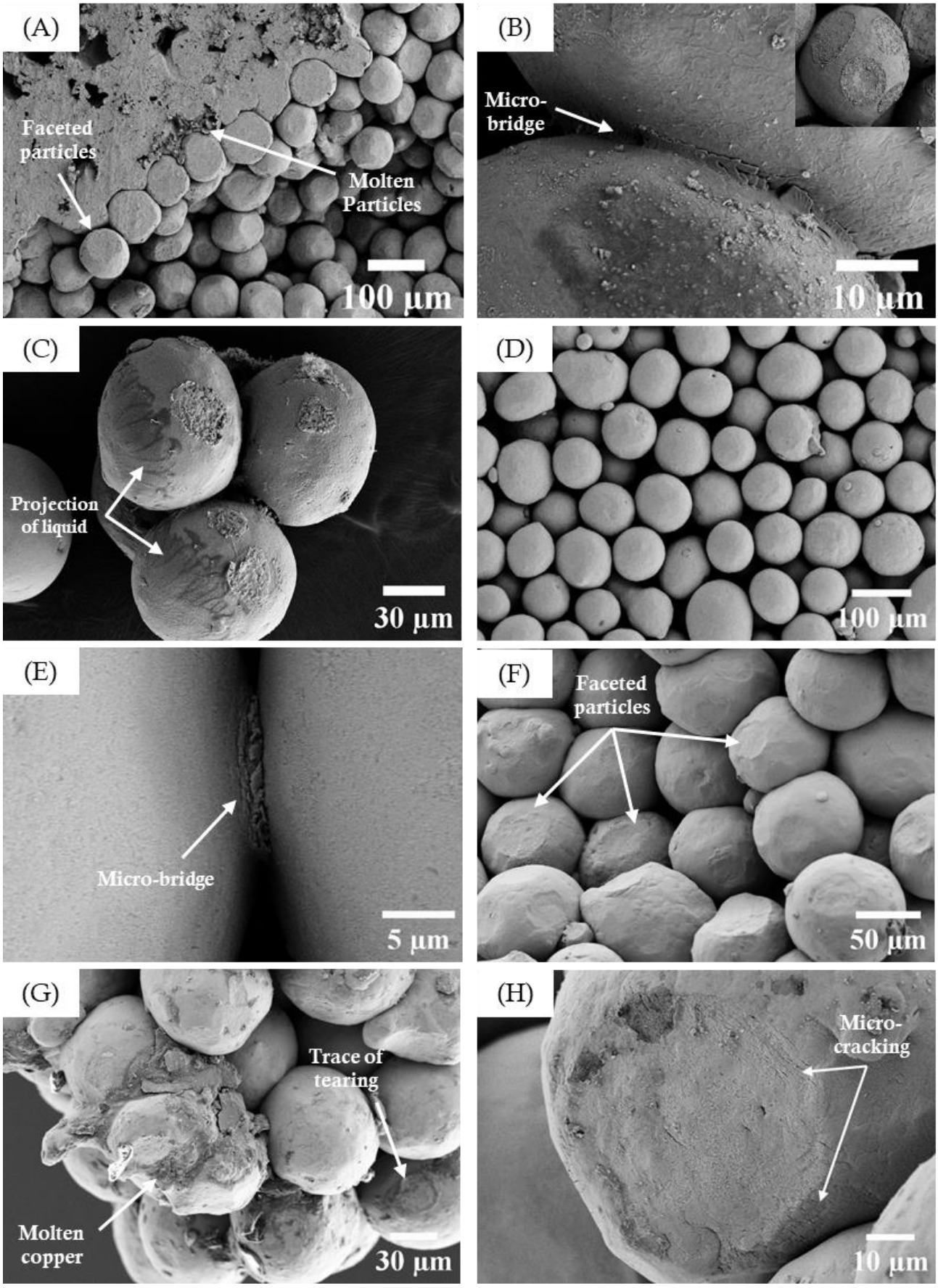

Figure 9: SEM observations of SPSed samples: after ignition of electrical transition within an insulating die under 41 MPa (A, B & C); treated at 250 °C for 5 min with a conductive die under 2.5 MPa (D & E) and 125 MPa (F, G & H).

3.3. *Discussion*

The behavior of a copper powder subjected to pulsed electric currents at high amperages was investigated. First, the coupling of the electric and magnetic fields was studied in a pulsed current demonstrator without thermal and mechanical stresses, *i.e.* at low temperature and very low stress. This allowed to highlight the effect of the pulse frequency on the consolidation mechanisms. Then, still at relatively low temperature (250 °C), the couplings between mechanical stress and pulsed current were analyzed in a commercial SPS apparatus by varying the applied stress. All the data collected here will be discussed in more detail in this section.

I) Electromagnetic coupling and induced current in SPS

Using the pulsed current demonstrator, the copper granular medium was subjected to pulsed currents with low frequencies of 6 and 40 Hz while limiting applied stress and nominal temperature. Using an insulating die, the critical time needed to initiate the Branly effect (*i.e.* abrupt electrical transition from an insulating state to a conducting state of the granular medium) was measured at various pulse frequencies. Increasing of the pulse frequency leads to a reduction of the time for the electrical transition by one decade. The increase of the pulse frequency gives rises to higher transient currents, *i.e.* higher dI/dt (I for current) as shown in ***Figure 1*** while the maximum current values remain roughly identical. It results that the current pulses are consequently a source of EM fields that may be absorbed by the granular medium. By virtue of the Faraday law, local electric fields are induced which may ignite the oxide layer breakdown. Therefore, they improve the metallic electrical contact between powder grains and allow a current density to establish. At last, owing to an electro-thermal coupling at the metallic microcontacts and according to the Kohlrausch equation given by $T_m^2 - T_0^2 = U^2/4L$ where T_m is the maximum temperature at the microcontact, T_0 the ambient temperature, L the Lorentz constant (2.45×10^{-8} V^2 / K^2) and U the local voltage due to local electric fields [39,40], the contact temperature may increase beyond the melting temperature because of the current density flowing through the contact. It results that a magnetic pinch in the electrically conductive liquid phase can occur bringing about Lorentz forces that can displace and even spray the molten liquid [23]. Increasing the frequency while keeping the maximum current constant increases the numbers of pulses per second and also the value of dI/dt, both effects accelerating the electrical transition.

Once the electrical transition has been obtained, the current flow within the stack ($I_{RMS} \approx 55$A after transition, *i.e.* a current density of 70 A/cm²) leads to a strong consolidation. These experiments have shown that the frequency of pulses has a major effect on the initiation of the Branly effect.

II) Reinforcement of the Branly effect in SPS by coupling between pulsed current and mechanical stress

As mentioned in the introduction, the beneficial effect of pulsed current in SPS is the subject of controversy in the literature. Many authors [29–32,34] have observed, on the basis of SEM and TEM observations, a phenomenon of surface cleaning and early elimination of the oxide layer at the interfaces between particles. They attribute this cleaning of the interparticle microcontacts to the flow of the pulsed current, which would cause processes ranging from local overheating to dielectric breakdown. This interface-cleaning phenomenon would favor the formation of interparticle necks during the initial stages of densification.

In the present work, the electrical behavior of the copper powder and the consolidation mechanisms initiated during the early stages of SPS treatments were studied in an instrumented SPS apparatus. Variable stress tests, with an insulating or conducting die, were conducted to investigate the electro-magneto-thermo-mechanical couplings. The SPS treatment of the copper powder at a very low temperature of 250°C under a high stress of 125 MPa (in a conductive die) led to a consolidated and conductive granular stack. The microstructural analysis revealed the presence of molten copper and faceted particles (contact surfaces of 30 µm diameter) due to the load applied during the SPS test. In addition, cracking of the oxide layer inside and at the periphery of these facets was observed. The microstructure is also characterized by the presence of micro-welds (25 to 30 µm in diameter) distributed in a non-homogeneous way in the stack; at the level of these micro-welds, the oxide layer is eliminated. In agreement with the results of Collet *et al.* [37], the increase in stress leads to a marked decrease in the temperature corresponding to the start of consolidation (500-700°C under 28 MPa according to [37] *vs.* 250 °C under 125 MPa here). However, the presence of molten copper for a macroscopic sample temperature around 250°C suggests the existence of a local overheating phenomenon within the stack, induced by the current flow. Besides, the hypothesis of Collet *et al.* in which the oxide is "repressed" from the interfaces by a thermomechanical effect seems incompatible with the low macroscopic temperature imposed here. Moreover, the oxide layer remains at the level of the formed facets, and is eliminated only at the level of the few micro-welds observed. The presence of inhomogeneously distributed microwelds suggests current flow along some discrete paths through the granular medium. The existence of discrete electrical conduction paths within metallic granular media has been demonstrated by Creyssels *et al.* [41] during the experimental mapping of conduction paths in a 2D stack of stainless steel balls subjected to isotropic compression. Finally, as shown here, the Branly effect and the associated elimination of the oxide layer at the interfaces are favored by the mechanical loading due to the increase in the interparticle contact surfaces and also to the damage by microcracking of the oxide layer.

In conclusion, the experiments under pulsed current carried out here have made it possible to well understand the mechanisms of electrical conduction within a granular copper medium. The results obtained highlight the importance of the coupling between current and mechanical stress on the initiation of the Branly effect. The parameters affecting the initiation of the Branly effect in SPS are: i) the imposed current generating intense local heating at the level of a few discrete current conduction paths (these conduction paths amplify and branch out with increasing current and stress [41]); ii) the frequency and amplitude of the pulses which generate induced current by electromagnetic effects (added to the imposed external current); iii) the mechanical stress which increases the interparticle contact surfaces and causes damage by microcracking of the insulating oxide layer. The Branly effect highlighted here generates the formation of micro-welds between the particles and thus participates in the initiation of the consolidation of the granular stack in SPS.

4. Conclusion

This work was devoted to the study of the coupling of multiple physical fields applied in SPS on the specific sintering mechanisms induced. In particular, the effects of electric and magnetic fields generated by the pulsed character of the current were studied implementing two complementary experimental enclosures: a demonstrator equipped with a modulable pulsed current generator and a commercial SPS device. A “model” copper powder, composed of spherical copper particles with a mono-disperse particle size distribution (average diameter of 87.5 µm), was used. Insulating and conductive dies were used to force or not the flow of the current within the granular medium. Mechanical stress level was changed to analyze coupling effects with applied pulsed current.

First, a demonstrator equipped with a modulable pulsed electric current generator has allowed to analyze, at low temperature and low stress, the effects related to the flow of a pulsed electric current by controlling and modulating the shape of the applied electric wave (*i.e.* shape, frequency, amplitude). An abrupt electrical transition from an insulating to a conductive state is observed in the granular copper medium, known as Branly effect. Increasing the frequency of the pulses leads to a reduction by one decade of the time to obtain the electrical transition. The microstructural observations after application of the pulsed current reveal a strong consolidation, with micro-bridges of 20 to 35 µm in diameter. This study showed that the frequency of the pulses has a major effect on the initiation of the Branly effect. The pulsed character of the current involves EM effects and probably induced currents, which add to the applied currents.

In addition, a commercial SPS device was used to investigate the combined effects of temperature and mechanical stress to the imposed electric and magnetic fields. A specific thermal and electrical instrumentation was used to monitor the electrical behavior of the copper powder. SPS tests were

conducted to study the electrical behavior of the copper powder during variable stress tests in order to understand the consolidation mechanisms initiated during the early stages of SPS treatment. Under low stress and low temperature (250 °C), microstructural analysis revealed the localized presence of micro-bridges of 10 µm in diameter. This suggests the partial initiation of the electrical transition under these conditions. Under a high stress of 125 MPa and at low temperature (250 °C), the granular stack was consolidated and became conductive. This observation leads to conclude that the Branly effect is induced during the early stage of SPS treatment. The microstructural analysis by SEM revealed the presence of large micro-bridges, molten copper and faceted particles due to the mechanical load applied in SPS. The coupling between pulsed current and mechanical stress promotes densification by increasing the interparticle contact areas and microcracking of the insulating oxide layer. This combination allows the generation of overheating (or even local melting) at the interparticle interfaces, which initiates densification.

These deep investigations have led to the identification of unconventional mechanisms during the early stages of SPS treatment, *i.e.* Branly effect (electrical transition) associated with local overheating and dielectric breakdown (destruction of the insulating oxide layer at interparticle micro-contacts). Then, micro-welds are formed, creating privileged paths for the flow of the pulsed current and thus improving the densification kinetics. These experimental results allow to deduce that the sintering mechanisms are significantly modified by the flow of the pulsed current in SPS.

According to this work, the initiation of the Branly effect and the involved consolidation mechanisms within metal powders are promoted both by the pulsed nature of the current, also by the application of high mechanical stress and finally by forcing the current to flow through the granular medium by means of an insulating die. Acceleration of consolidation and densification of metal powders using SPS process can thus be achieved by adapting the tooling to combine the use of an insulating die with the application of high mechanical stresses.

Funding

This work was carried out thanks to the financial support of the French "Nouvelle-Aquitaine Region" within the framework of the SMICMES project (convention n° 2019-1R10122) and the grant of A. Aliouat.

Declaration of competing interests

The authors declare that they have no known competing financial interests or personal relationships that could have appeared to influence the work reported in this paper

Acknowledgments

The authors thank Marion Vandenhende (University of Limoges-IRCER) for SPS measurements.

References

[1] R. Orrù, R. Licheri, A.M. Locci, A. Cincotti, G. Cao, Consolidation/synthesis of materials by electric current activated/assisted sintering, Mater. Sci. Eng. R Rep. 63 (2009) 127–287. https://doi.org/10.1016/j.mser.2008.09.003.

[2] O. Guillon, J. Gonzalez-Julian, B. Dargatz, T. Kessel, G. Schierning, J. Räthel, M. Herrmann, Field-Assisted Sintering Technology/Spark Plasma Sintering: Mechanisms, Materials, and Technology Developments, Adv. Eng. Mater. 16 (2014) 830–849. https://doi.org/10.1002/adem.201300409.

[3] M. Yu, S. Grasso, R. Mckinnon, T. Saunders, M.J. Reece, Review of flash sintering: materials, mechanisms and modelling, Adv. Appl. Ceram. 116 (2017) 24–60. https://doi.org/10.1080/17436753.2016.1251051.

[4] M. Abedi, A. Asadi, S. Vorotilo, A.S. Mukasyan, A critical review on spark plasma sintering of copper and its alloys, J. Mater. Sci. 56 (2021) 19739–19766. https://doi.org/10.1007/s10853-021-06556-z.

[5] Z.A. Munir, U. Anselmi-Tamburini, M. Ohyanagi, The effect of electric field and pressure on the synthesis and consolidation of materials: A review of the spark plasma sintering method, J. Mater. Sci. 41 (2006) 763–777. https://doi.org/10.1007/s10853-006-6555-2.

[6] Z.-Y. Hu, Z.-H. Zhang, X.-W. Cheng, F.-C. Wang, Y.-F. Zhang, S.-L. Li, A review of multi-physical fields induced phenomena and effects in spark plasma sintering: Fundamentals and applications, Mater. Des. 191 (2020) 108662. https://doi.org/10.1016/j.matdes.2020.108662.

[7] U. Anselmi-Tamburini, S. Gennari, J.E. Garay, Z.A. Munir, Fundamental investigations on the spark plasma sintering/synthesis process: II. Modeling of current and temperature distributions, Mater. Sci. Eng. A. 394 (2005) 139–148. https://doi.org/10.1016/j.msea.2004.11.019.

[8] P. Cavaliere, B. Sadeghi, A. Shabani, Spark Plasma Sintering: Process Fundamentals, in: P. Cavaliere (Ed.), Spark Plasma Sinter. Mater. Adv. Process. Appl., Springer International Publishing, Cham, 2019: pp. 3–20.

[9] R. Chaim, G. Chevallier, A. Weibel, C. Estournès, Grain growth during spark plasma and flash sintering of ceramic nanoparticles: a review, J. Mater. Sci. 53 (2018) 3087–3105. https://doi.org/10.1007/s10853-017-1761-7.

[10] H. Ding, Z. Zhao, J. Jin, L. Deng, P. Gong, X. Wang, Densification mechanism of Zr-based bulk metallic glass prepared by two-step spark plasma sintering, J. Alloys Compd. 850 (2021) 156724. https://doi.org/10.1016/j.jallcom.2020.156724.

[11] B. Huang, L.D. Chen, S.Q. Bai, Bulk ultrafine binderless WC prepared by spark plasma sintering, Scr. Mater. 54 (2006) 441–445. https://doi.org/10.1016/j.scriptamat.2005.10.014.

[12] J. Zhao, T. Holland, C. Unuvar, Z.A. Munir, Sparking plasma sintering of nanometric tungsten carbide, Int. J. Refract. Met. Hard Mater. 27 (2009) 130–139. https://doi.org/10.1016/j.ijrmhm.2008.06.004.

[13] K. Sairam, J.K. Sonber, T.S.R.Ch. Murthy, C. Subramanian, R.K. Fotedar, P. Nanekar, R.C. Hubli, Influence of spark plasma sintering parameters on densification and mechanical properties of boron carbide, Int. J. Refract. Met. Hard Mater. 42 (2014) 185–192. https://doi.org/10.1016/j.ijrmhm.2013.09.004.

[14] X. Li, D. Jiang, J. Zhang, Q. Lin, Z. Chen, Z. Huang, Densification behavior and related phenomena of spark plasma sintered boron carbide, Ceram. Int. 40 (2014) 4359–4366. https://doi.org/10.1016/j.ceramint.2013.08.106.

[15] G. Victor, Y. Pipon, N. Bérerd, N. Toulhoat, N. Moncoffre, N. Djourelov, S. Miro, J. Baillet, N. Pradeilles, O. Rapaud, A. Maître, D. Gosset, Structural modifications induced by ion irradiation and temperature in boron carbide B4C, Nucl. Instrum. Methods Phys. Res. Sect. B Beam Interact. Mater. At. 365 (2015) 30–34. https://doi.org/10.1016/j.nimb.2015.07.082.

[16] X. Wei, C. Back, O. Izhvanov, O.L. Khasanov, C.D. Haines, E.A. Olevsky, Spark Plasma Sintering of Commercial Zirconium Carbide Powders: Densification Behavior and Mechanical Properties, Materials. 8 (2015) 6043–6061. https://doi.org/10.3390/ma8095289.

[17] H. Laadoua, N. Pradeilles, R. Lucas, S. Foucaud, W.J. Clegg, Preparation of ZrC/SiC composites by using polymer-derived ceramics and spark plasma sintering, J. Eur. Ceram. Soc. 40 (2020) 1811–1819. https://doi.org/10.1016/j.jeurceramsoc.2019.12.019.

[18] Y. Zhao, M. Wang, Effect of sintering temperature on the structure and properties of polycrystalline cubic boron nitride prepared by SPS, J. Mater. Process. Technol. 209 (2009) 355–359. https://doi.org/10.1016/j.jmatprotec.2008.02.005.

[19] J. Wan, R.-G. Duan, A.K. Mukherjee, Spark plasma sintering of silicon nitride/silicon carbide nanocomposites with reduced additive amounts, Scr. Mater. 53 (2005) 663–667. https://doi.org/10.1016/j.scriptamat.2005.05.037.

[20] M. Coëffe-Desvaux, N. Pradeilles, P. Marchet, M. Vandenhende, M. Joinet, A. Maître, Comparative Study on Electrical Conductivity of CeO2-Doped AlN Ceramics Sintered by Hot-Pressing and Spark Plasma Sintering, Materials. 15 (2022) 2399. https://doi.org/10.3390/ma15072399.

[21] T. Misawa, N. Shikatani, Y. Kawakami, T. Enjoji, Y. Ohtsu, H. Fujita, Observation of internal pulsed current flow through the ZnO specimen in the spark plasma sintering method, J. Mater. Sci. 44 (2009) 1641–1651. https://doi.org/10.1007/s10853-008-2906-5.

[22] P. Guyot, V. Rat, J.F. Coudert, F. Jay, A. Maître, N. Pradeilles, Does the Branly effect occur in spark plasma sintering?, J. Phys. Appl. Phys. 45 (2012) 092001. https://doi.org/10.1088/0022-3727/45/9/092001.

[23] H. Deng, J. Dong, F. Boi, T. Saunders, C. Hu, S. Grasso, Magnetic Field Generated during Electric Current-Assisted Sintering: From Health and Safety Issues to Lorentz Force Effects, Metals. 10 (2020) 1653. https://doi.org/10.3390/met10121653.

[24] J.R. Friedman, J.E. Garay, U. Anselmi-Tamburini, Z.A. Munir, Modified interfacial reactions in Ag–Zn multilayers under the influence of high DC currents, Intermetallics. 12 (2004) 589–597. https://doi.org/10.1016/j.intermet.2004.02.005.

[25] Z. Trzaska, J.-P. Monchoux, Electromigration experiments by spark plasma sintering in the silver–zinc system, J. Alloys Compd. 635 (2015) 142–149. https://doi.org/10.1016/j.jallcom.2015.02.122.

[26] S. Deng, R. Li, T. Yuan, P. Cao, Effect of electric current on crystal orientation and its contribution to densification during spark plasma sintering, Mater. Lett. 229 (2018) 126–129. https://doi.org/10.1016/j.matlet.2018.07.001.

[27] G. Maizza, G.D. Mastrorillo, S. Grasso, H. Ning, M.J. Reece, Peltier effect during spark plasma sintering (SPS) of thermoelectric materials, J. Mater. Sci. 52 (2017) 10341–10352. https://doi.org/10.1007/s10853-017-1188-1.

[28] Y. Kim, C. Shin, T. Kim, S.-W. Kang, Inhomogeneity in thermoelectrics caused by Peltier effect-induced temperature gradient during spark plasma sintering, Scr. Mater. 158 (2019) 46–49. https://doi.org/10.1016/j.scriptamat.2018.08.024.

[29] O. Yanagisawa, H. Kuramoto, K. Matsugi, M. Komatsu, Observation of particle behavior in copper powder compact during pulsed electric discharge, Mater. Sci. Eng. A. 350 (2003) 184–189. https://doi.org/10.1016/S0921-5093(02)00726-8.

[30] X. Song, X. Liu, J. Zhang, Neck Formation and Self-Adjusting Mechanism of Neck Growth of Conducting Powders in Spark Plasma Sintering, J. Am. Ceram. Soc. 89 (2006) 494–500. https://doi.org/10.1111/j.1551-2916.2005.00777.x.

[31] C.S. Bonifacio, T.B. Holland, K. van Benthem, Evidence of surface cleaning during electric field assisted sintering, Scr. Mater. 69 (2013) 769–772. https://doi.org/10.1016/j.scriptamat.2013.08.018.

[32] M. Wu, Y. Yang, G. Yang, K. Huang, D. Yin, Direct evidence for surface cleaning mechanism during field-activated sintering, J. Alloys Compd. 784 (2019) 975–979. https://doi.org/10.1016/j.jallcom.2019.01.035.

[33] A. Aliouat, G. Antou, V. Rat, N. Pradeilles, P.-M. Geffroy, A. Maître, Investigation of Electrical Transitions in the First Steps of Spark Plasma Sintering: Effects of Pre-Oxidation and Mechanical Loading within Copper Granular Media, Materials. 15 (2022) 4096. https://doi.org/10.3390/ma15124096.

[34] S. Diouf, A. Fedrizzi, A. Molinari, A fractographic and microstructural analysis of the neck regions of coarse copper particles consolidated by spark plasma sintering, Mater. Lett. 111 (2013) 17–19. https://doi.org/10.1016/j.matlet.2013.08.056.

[35] Z.-H. Zhang, Z.-F. Liu, J.-F. Lu, X.-B. Shen, F.-C. Wang, Y.-D. Wang, The sintering mechanism in spark plasma sintering – Proof of the occurrence of spark discharge, Scr. Mater. 81 (2014) 56–59. https://doi.org/10.1016/j.scriptamat.2014.03.011.

[36] C. Romaric, L.G. Sophie, N. Foad, C. Frédéric, B. Guillaume, F. Gilbert, C. Jean-Marc, B. Frédéric, Effect of current on the sintering of pre-oxidized copper powders by SPS, J. Alloys Compd. 692 (2017) 478–484. https://doi.org/10.1016/j.jallcom.2016.08.191.

[37] R. Collet, S. Le Gallet, F. Charlot, S. Lay, J.-M. Chaix, F. Bernard, Effect of Electric Current on SPS Densification of Spherical Copper Powder, J. Manuf. Mater. Process. 5 (2021) 119. https://doi.org/10.3390/jmmp5040119.

[38] J. Diatta, G. Antou, F. Courreges, M. Georges, N. Pradeilles, A. Maître, Effect of the current pulse pattern during heating in a spark plasma sintering device: Experimental and numerical modeling approaches, J. Mater. Process. Technol. 246 (2017) 93–101. https://doi.org/10.1016/j.jmatprotec.2017.03.004.

[39] E. Falcon, B. Castaing, M. Creyssels, Nonlinear electrical conductivity in a 1D granular medium, Eur. Phys. J. B - Condens. Matter Complex Syst. 38 (2004) 475–483. https://doi.org/10.1140/epjb/e2004-00142-9.

[40] E. Falcon, B. Castaing, Electrical conductivity in granular media and Branly's coherer: A simple experiment, Am. J. Phys. 73 (2005) 302–307. https://doi.org/10.1119/1.1848114.

[41] M. Creyssels, S. Dorbolo, A. Merlen, C. Laroche, B. Castaing, E. Falcon, Some aspects of electrical conduction in granular systems of various dimensions, Eur. Phys. J. E. 23 (2007) 255–264. https://doi.org/10.1140/epje/i2006-10186-9.